An Acoustic Emission based Structural Health Monitoring Approach to Railway Axles

Michele Carboni

Politecnico di Milano, Dept. Mechanical Engineering, Italy, michele.carboni@polimi.it

Abstract

Considering railway axles, classical fatigue damage can occur at the body as a consequence of corrosion or ballast impacts, while fretting damage can occur as a result of micro-sliding between the wheel assembly and the press-fit seat. As safety critical components, railway axles, whose failure can lead to unacceptable human losses, are periodically inspected by means of well-established non-destructive techniques (typically ultrasonic and magnetic particle inspections) usually requiring expensive service interruptions. On the contrary, as shown within the aeronautical field, a condition-based maintenance can improve the safety and at the same time minimize costs respect to scheduled inspections. This paper investigates the feasibility of an Acoustic Emission based Structural Health Monitoring approach applied to railway axles subjected to classical and fretting fatigue damages. Experiments were performed on full-scale axles using a Vitry test rig, i.e. a three point bending test, with one acoustic-emission sensor coupled at the free end of the axle. Results are found to be consistent with damage evolution.

1. Introduction

The present scenario (1) of European railway applications shows a tendency towards new maintenance and monitoring procedures for in-service solid axles, with the aim to define higher safety levels and, at the same time, to optimize the total cycle life cost of the wheel-set. In particular, during service of railway axles, corrosion-fatigue, ballast impacts and fretting fatigue damages can occur and trigger crack initiation with consequent failure (2). For this reason, railway axles, whose failure can lead to unacceptable human losses, are periodically inspected by means of well-established non-destructive techniques (typically ultrasonic and magnetic particle inspections) usually requiring expensive service interruptions. From this point of view, as shown within the aeronautical field (3), switching to a condition-based maintenance can improve the safety and, at the same time, minimize costs with respect to scheduled inspections.

Nowadays, the applied structural health monitoring (SHM) techniques are, in general, based on different physical phenomena (4): dynamic modal data, electromechanical impedance, static parameters (displacement field, strain gauges, optical fibres etc.), acoustic emission (AE) and elastic waves. In particular, AE (5) is generated by developing damages in terms of elastic waves and it is an effective way of localization via triangulation and of evaluation of failure behaviour. AE technology is, then, a passive non-destructive technique applying a continuous monitoring, which makes

possible to evaluate the possible development of damage in real time. This aspect makes it potentially more convenient than common inspection procedures based on the "Damage Tolerance" approach (1), according to which axles must be stopped and checked at least two times before possible failure can occur, with consequent inconveniences in terms of both down-time and money. However, the employment of acoustic emission for railway axles monitoring is an innovative application, since the majority of the cases, in railway field, concerns the monitoring of rail-wheel contact (6) and the detection of faults in axle bearings (7) and tracks (8).

This paper investigates the feasibility of an Acoustic Emission based Structural Health Monitoring system applied to railway axle subjected to fretting fatigue damage. Experiments were performed on a full-scale axle using a Vitry test rig, i.e. a three point rotating bending test, with an acoustic-emission sensor coupled at the free end of the axle. Preliminary results are introduced and are found to be consistent with damage evolution.

2. Full-scale fretting fatigue test

The full-scale experiment was carried out according to the experimental set-up suggested in EN 13261 for testing critical region F3, i.e. the "limit under the fitted areas (for solid axle)" (9). In particular, the considered full-scale specimen is representative of a solid axle manufactured in EA4T steel grade (quenched and tempered 25CrMo4 alloy) and its geometry is shown in Figure 1a. Moreover, with the aim of verifying the propagation attitude of pre-existing defects under the press-fit, four artificial defects were machined under the hub, as shown in Figure 1b. They were obtained by EDM on one side of the wheel seat, at a distance of 10 mm from the edge, equally spaced with a circumferential length of 75° each and a depth of 350 μm. Their shape and depth were confirmed by a following SEM analysis: Figure 1b shows an example of lapped section of one of the artificial defects.

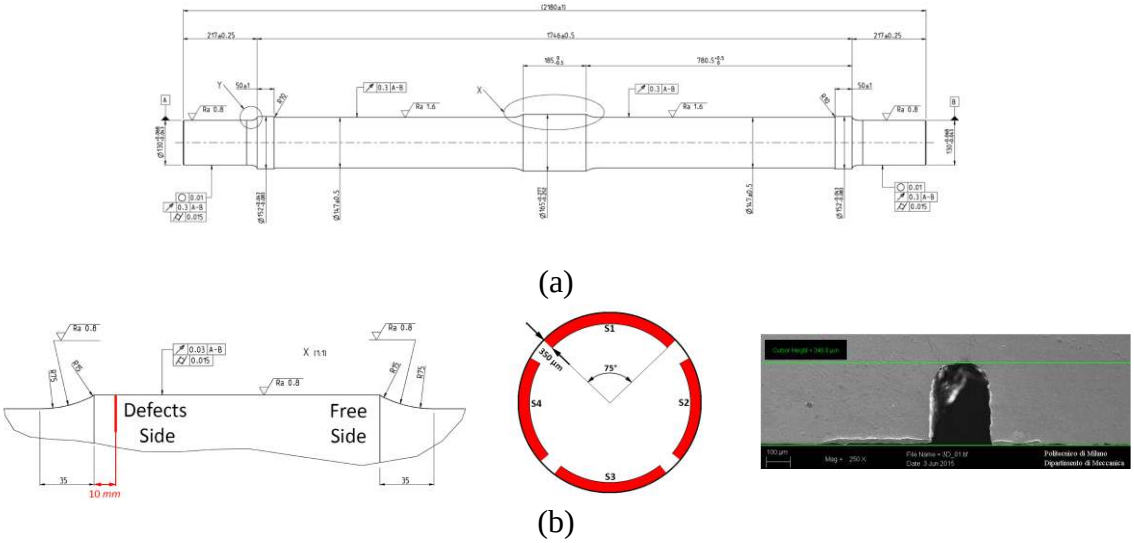

Figure 1. Full-scale specimen: a) technical drawing; b) artificial defects located under the press-fit.

The test was carried out by the Vitry test bench available at the labs of the Dept. Mechanical Engineering at Politecnico di Milano (Figure 2). This is a special bench able to apply three point rotating bending conditions to full-scale specimens. The hydraulic actuator has a maximum load capacity of 250 kN and a three-phase asynchronous motor can impose a maximum rotational speed of 1000 rpm.

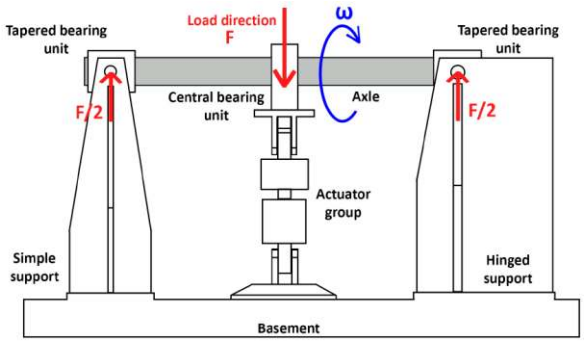

Figure 2. Static scheme of the Vitry test bench for full-scale axles.

Previous studies showed (10) that, for the considered material and axle geometry, the fretting fatigue limit is approximately 120 MPa. In order to check such a conclusion, two different nominal stress levels were applied, during the test, at the section of the press-fit seat where artificial defects were located: first, 108 MPa were applied for $1.5x10^7$ cycles without observing any macroscopic clue of damage, then 135 MPa were applied for about 6.5x106 cycles at which failure occurred. In particular, failure was detected by an ultrasonic phased array system applied, during the test, at suitable interruptions.

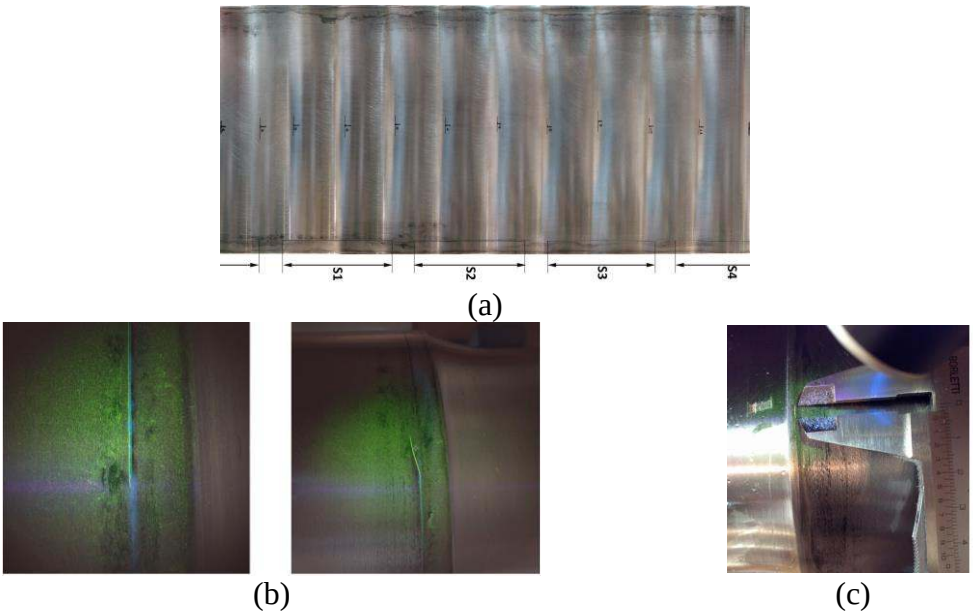

(a)

(b) (c)

Figure 3. Surface inspection of the tested press-fit seat: a) 2D map visual testing; b) and c) fluorescent magnetic particle testing.

The specimens was, then, disassembled and the press-fit seat inspected by visual testing (2D map, Figure 3a) and fluorescent magnetic particle testing (Figure 3b and 3c). As can be seen, two cracks developed during the test: the first one (Figure 3b) initiated at

defect S1 and extended from both sides of it, while the second much smaller one (Figure 3c) initiated at the free side of the seat (3 mm from the edge) with circumferential extension of 4 mm.

3. Structural health monitoring by acoustic emission

The experimental set-up for AE structural health monitoring consisted (Figure 4) in a Vallen AE control unit AMSY-6 with eight channels, a piezoelectric sensor Vallen VS150-M at 150 kHz, a Pre-amplifier Vallen AEP4 at 34dB and a sliding contact to drive the signal from the piezoelectric sensor and the pre-amplifier, both rotating along with the axle, to the control unit. The sensor was coupled to the axle by means of a silicone couplant. The control unit acquired also the signals of the applied load and of the number of cycles so that each event could be precisely associated to its number of fatigue cycles and to the load.

Unfortunately, due to the bench configuration, just one sensor could be adopted during the test because, of the two flat ends of the full-scale axle, one is not accessible since it is connected through a gear to the motor pulley aimed at the rotational speed transfer. This means no localization of events could be carried out, losing a lot of useful information for the interpretation of results.

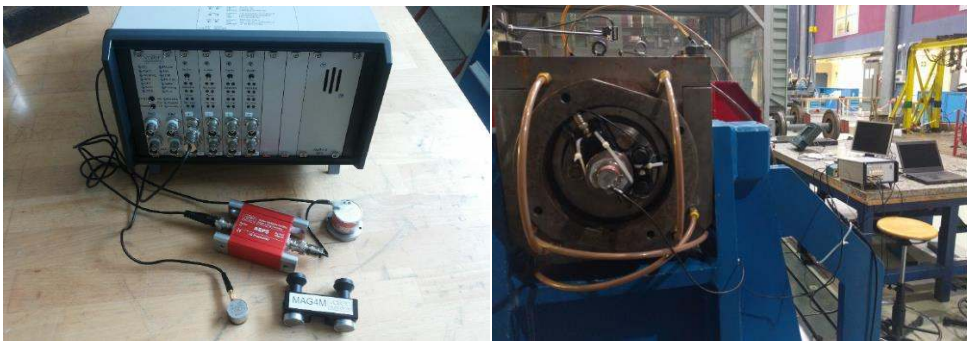

Figure 4. Experimental set-up for AE structural health monitoring of the axle.

In order to check the acoustic contact of the sensor, many calibration acquisitions were carried out by the pencil lead break (PLB) test (5). In particular, PLBs were applied on the axle surface starting from the nearest possible location to the sensor (267 mm) to the furthest (1813 mm) at regular length distances of 100 mm. All the signals originated by PLBs exhibited a clear burst waveform with amplitude of 70 dB (Figure 5).

A characterization of environmental noise was, then, carried out (Figure 5). First, the axle was put in rotation at the test speed (509 rpm) without any applied load: in this condition, acquired acoustic emission signals are just related to random noise (from the electric motor, bearings …). Then, electro-magnetic interference was acquired plugging and unplugging the set-up cables. Finally, the interference of the moving bridge crane of the lab was acquired, as well. All the acquired data allowed to properly set the acquisition threshold, which was set to 69 dB, in order to include signals similar to PLBs and reduce as much as possible the amount of useless data.

During the test, for all the recorded events, the experimental set-up automatically provided a set of numerical features suitable for describing the raw signal: the channel acquiring the signal (CHAN), amplitude (A), rise time (RT), duration (D), counts (CNTS), energy (E), root mean square (RMS), threshold (THR), number of cycles (PCTA), FLAG for indicating special conditions during a hit and TRAI to enumerate all the hits with an associated transient data. Indeed, AMSY-6 allowed also recording the waveform of any hit (transient recorder) and analysing it in the frequency domain (11).

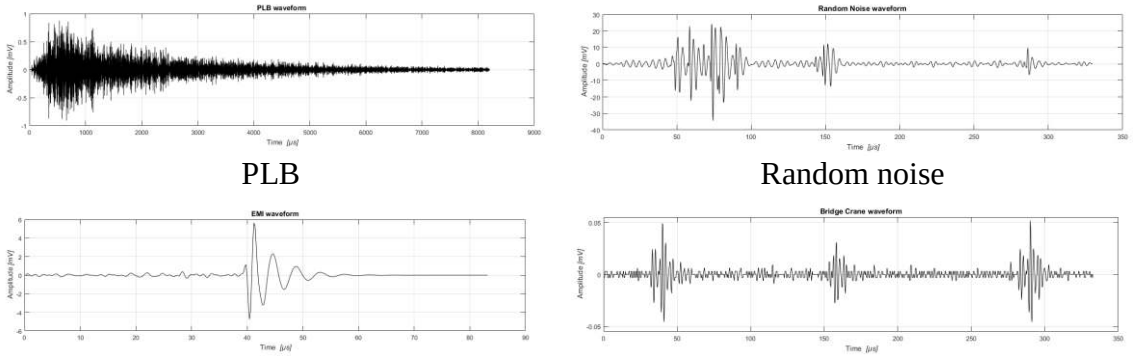

PLB | Random noise

Electro-magnetic interference | Bridge crane

Figure 5. Examples of waveforms acquired from the environment.

Figure 6 shows the complete raw data (a total of 660.000 hits) acquired during the full-scale test and plotted in terms of amplitude vs. cycles and cumulated energy vs. cycles. As can be seen, the amount of recorded events is large and this is the consequence of the high background noise level and the long duration of the test. Consequently, a general real-time criterion aimed at the identification of failure mechanisms seems difficult to be applied and the performance of a post-processing algorithm has been investigated, as described in the following.

4. Interpretation of acoustic emission results by an unsupervised artificial neural network

Pattern recognition techniques are considered a suitable tool to identify distinct types of AE sources based on a multitude of features obtained from the recorded signals (12). It also worth remarking the formation of AE signal clusters depends sensitively on the experimental set-up, the geometry of the specimen and the possible existence of other AE sources not correlated to specimen failure (13). In the literature, to face this kind of classification problems in the case of AE, the adoption of unsupervised (14) algorithms is suggested (5). Due to the known good performance (5), an unsupervised artificial neural network (ANN) algorithm, based on the Self-Organizing Map (SOM) (15), was adopted for the present case. The unsupervised nature of this approach does not require to know the output a priori, but allows to arrange its architecture according to the input: this is particularly useful for the big amount of AE data to be analyzed for the fretting fatigue damage of axles.

The adopted SOM had a hexagonal lattice with a sheet structure, with a Gaussian neighborhood function. The observation of the U-Matrix allowed appreciating some degree of separation among groups of different neurons. In this regard, it could be

therefore possible to create a small number of clusters through simple clustering algorithms, such as the k-means one (15). However, a big problem consisted in selecting the optimal number of clusters a priori. Indeed, once the SOM is trained and the U-Matrix displayed, the decision of the number of classes in which the input dataset must be divided stands to the user. To address this issue, the automatic k-SOM classifier algorithm, developed by Davide Crivelli (16) in a research on composite materials, was adopted. This approach evaluates the best performing number of clusters a priori, taking as a reference a few quality-clustering indexes in a straightforward and automated way. More in detail, after training the SOM, the U-Matrix is clustered with the k-means algorithm using a number of classes c ranging from $c_{min} = 2$ to $c_{max} = 15$. The clustering quality is then evaluated through three performance indexes: Davies-Bouldin (17), Silhouette (18) and Calinski-Harabasz (19). The use of multiple indexes allows overcoming the limitations and characteristics of every single parameter. These entire features make the approach implementable in any AE based structural health monitoring systems.

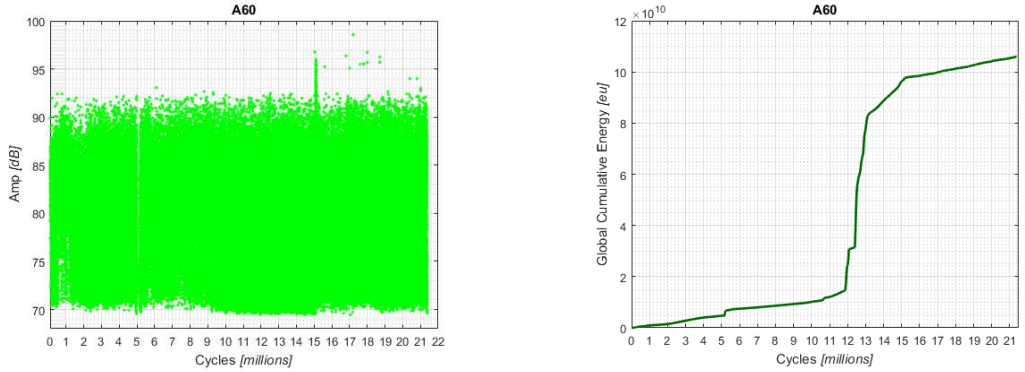

Figure 6. Complete AE raw data acquired during the full-scale test.

The application of the automatic k-SOM algorithm to fretting fatigue AE data identified the best number of classes as $c_{best} = 2$ with a correspondent aggregate index level $L_i = 41$ (Figure 7a). Figure 7b, instead, shows the comparison of the obtained two classes in terms of the Duration vs. Counts chart: Class 1 contains about 105.000 hits, while Class 2 about 565.000 hits. As can be seen, it is the largest class (Class 2) to be characterized by the higher values of duration and counts, a condition suggesting (Figure 5) this class is the one more probably related to damage, while the other one (Class 1) to noise.

The same conclusion is more strongly supported by the clustered cumulative charts shown in Figure 8, which reveal a clearly increasing constant trend of Class 1 with time: it contains a small number of signals with a low energy content and seems to well represent the expected behaviour of a continuous background noise. Class 2, instead, includes the highest percentage of signals with also the highest cumulated energy located over a rather small range of fretting fatigue cycles: from the literature (20), it is known that crack initiation and final fracture present sudden and high accumulation of energy, while the propagation phase is almost silent. Since the final fracture phase of a crack initiated in a railway axle coincides with the failure of the whole axle, the sudden increment of energy shown in Figure 8 can only be associated to crack initiation. It can be concluded a limited number of crack initiations occurred during the test, since the sudden accumulations of energy are not in an evident number. This hypothesis finds

confirmation by the experimental observations carried out at the end of the test, since only two surface cracks could be found.

It can be concluded automatic k-SOM is able to distinguish between phenomena related to background noise (Class 1) and events related to damage mechanisms (Class 2).

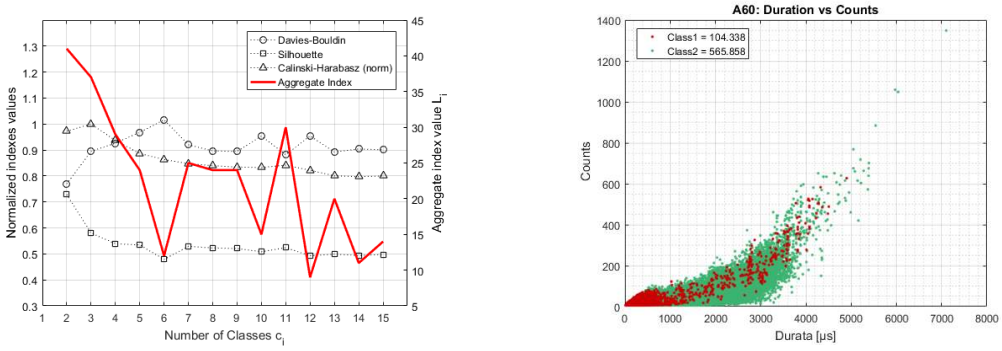

(a) (b)

Figure 7. Classification of AE data: a) indexes and definition of classes; b) automatic k-SOM results (Duration vs Counts chart).

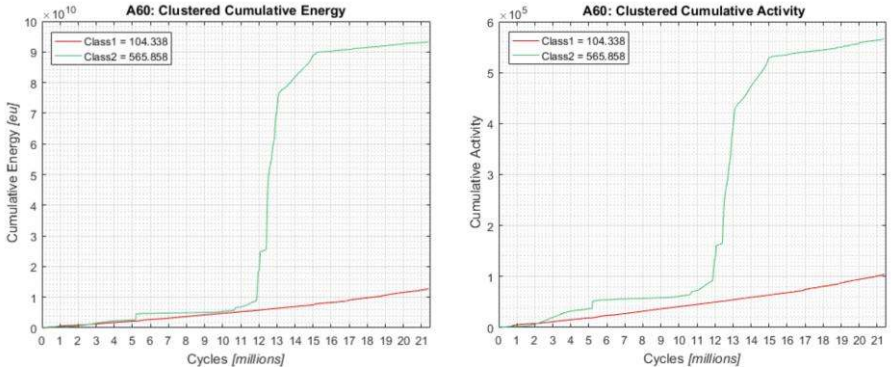

Figure 8. Automatic k-SOM results: clustered cumulative Energy (left) and Activity (right) charts.

4. Conclusions

In conclusion, it worth to highlight the usage of AE technology to monitor fretting fatigue tests on railway axles, besides being an innovative application, runs into a quantity of issues and criticalities implying the complex interpretation of the relationship between the damaging phenomena and the corresponding AE responses. Nevertheless, the application of suitable elaboration tools proved to be very encouraging for future developments.

Acknowledgements

The author would like to thank Prof. S. Beretta, Prof. S. Foletti (Dept. Mechanical Engineering – Politecnico di Milano) and Mr. S. Cantini (Lucchini RS SpA) for the useful discussion and Dr. A. Gianneo and Mr. S. Bertozzi for the active help given to the research. The author would like to thank the "PoliNDT" interdisciplinary laboratory for the acoustic emission equipment.

References

1. Cantini S, Beretta S.: Structural reliability assessment of railway axles, Lucchini RS Technical Series 4, 2011.
2. Beretta S., Carboni M.: Variable amplitude fatigue crack growth in a mild steel for railway axles: experiments and predictive models, Engineering Fracture Mechanics, Vol. 78, No. 5, 2011, 848–862.
3. Boller C.: Ways and options for aircraft structural health management, Smart Mater Struct, Vol. 10, 2001, 432–440.
4. Su Z., Ye L.: Identification of damage using Lamb waves: from fundamentals to applications. Springer Science & Business Media, 2009.
5. Ohtsu M.: Theory and Characteristics of Acoustic Emission, Morikita Pub., 1998.
6. Bollas K.: Acoustic emission inspection of rail wheels, J. Acoust. Emission, Vol. 28, 2010, 215–228.
7. Kaewkongka T.: A train bearing fault detection and diagnosis using acoustic emission, Engineering Solid Mechanics, Vol. 4, No. 2, 2016, 63–68.
8. Bruzelius K., Mba D.: An initial investigation on the potential applicability of Acoustic Emission to rail track fault detection, NDT & E International, Vol. 37, No. 7, 2004, 507–516.
9. EN 13261: Railway applications – wheelsets and bogies – axles – product requirements, CEN, 2009.
10. Verderio S., Salvador M.: Experimental and numerical analysis of fretting fatigue cracks propagation in railway axles, MSc Thesis, Politecnico di Milano, Milano, Italy, 2016.
11. Vallen System: AMSY-6 Operation Manual, Vallen Systeme GmbH, 2015.
12. Ramirez-Jimenez C.R.: Identification of failure modes in glass/polypropylene composites by means of the primary frequency content of the acoustic emission event, Composites Science and Technology, Vol. 64, No. 12, 2004, 1819–1827.
13. Sause M.G.R., Horn S.: Influence of specimen geometry on acoustic emission signals in fiber reinforced composites: FEM-simulations and experiments, Proceedings of the 29th European Conference on Acoustic Emission Testing, Vienna, Austria, 2010.
14. Anastasopoulos A.A., Philippidis T.P.: Clustering Methodologies for the evaluation of AE from Composites, J. of Acoustic Emission, Vol. 13, 1995.
15. Kohonen T.: The self-organizing map, Proceedings of the IEEE, Vol. 78, No. 9, 1990, 1464–1480.
16. Crivelli D.: Structural health monitoring with acoustic emission and neural networks, PhD thesis, Politecnico di Milano, Milano, Italy, 2014.
17. Davies D.L., Bouldin D.W.: A cluster separation measure, IEEE transactions on pattern analysis and machine intelligence, Vol. 2, 1979, 224–227.
18. Rousseeuw P.J.: Silhouettes: a graphical aid to the interpretation and validation of cluster analysis, Journal of computational and applied mathematics, Vol. 20, 1987, 53–65.
19. Calinski T., Harabasz J.: A dendrite method for cluster analysis, Communications in Statistics-theory and Methods, Vol. 3, No. 1, 1974, 1–27.
20. Marfo A., Chen Z., Li J.: Acoustic emission analysis of fatigue crack growth in steel structures, Journal of Civil Engineering and Construction Technology, Vol. 4, No. 7, 2013, 239–249.